Tests of a Full-Scale ITER Toroidal Interferometer and Polarimeter (TIP) Prototype on the DIII-D Tokamak[a)]

M. A. Van Zeeland[1], T. N. Carlstrom[1], D. K. Finkenthal[2], T. Akiyama[3], R.L. Boivin[1], A. Colio [2], D. Du[1], A. Gattuso[1], F. Glass[1], C. M. Muscatello[1], R. O'Neill[1], M. Smiley[1], J. Vasquez[1], M. Watkins[1], D. L. Brower[4], J. Chen[4], W. X. Ding[4], D. Johnson[5], P. Mauzey[1], M. Perry[6] C. Watts[7] and R. Wood[5]

[1)] *General Atomics, P.O. Box 85608 San Diego, California 92186-5608, USA*
[2)] *Palomar Scientific Instruments, San Marcos, CA 92069, USA*
[3)] *National Institute for Fusion Science, Gifu 509-5292, Japan*
[4)] *Dept. of Physics and Astron., Univ. of Calif. Los Angeles, CA 90095, USA*
[5)] *Princeton Plasma Phys. Lab. PO Box 451, Princeton, NJ 08543-0451, USA*
[6)] *Cal State University, San Marcos, CA, 92096, USA*
[7)] *ITER Organization, 13067 St. Paul Lez Durance Cedex, France*

A full-scale ITER toroidal interferometer and polarimeter (TIP) prototype, including an active feedback alignment system, has been installed and tested on the DIII-D tokamak. In the TIP prototype, a two-color interferometry measurement of line-integrated density is carried out at 10.59 μm and 5.22 μm using a CO_2 and Quantum Cascade Laser (QCL) respectively while a separate polarimetry measurement of the plasma induced Faraday effect is made at 10.59 μm. The TIP prototype is equipped with a piezo tip/tilt stage active feedback alignment system which minimizes noise in the measurement and keeps the diagnostic aligned throughout DIII-D discharges. The measured phase resolution for the polarimeter and interferometer are 0.05 Deg (100 Hz bandwidth) and 1.9 Deg (1 kHz bandwidth) respectively. The corresponding line-integrated density resolution for the vibration compensated interferometer is δnL=1.5×10^{18} m^{-2} and the magnetic field weighted line-integrated density from the polarimeter is δnBL=1.5×10^{19} Tm^{-2}. Both interferometer and polarimeter measurements during DIII-D discharges compare well to expectations based on calculations using Thomson scattering measured density profiles and magnetic equilibrium reconstructions. Additionally, larger bandwidth interferometer measurements show the diagnostic is a sensitive monitor of core density fluctuations with demonstrated measurements of Alfvén eigenmodes, tearing modes and sawteeth.

I. INTRODUCTION

The primary system planned for real-time density control in ITER is the five channel combined toroidal interferometer and polarimeter (TIP). TIP will also contribute to density profile reconstruction and play a secondary role as a diagnostic of core density fluctuations.[1] Initial design studies of the TIP based on CO_2 and CO lasers were carried out in 1998[2,3] and, in 2013 a more detailed design was published[4]. In 2015-2016, a TIP lab prototype with the scale of that expected in ITER was constructed and tested[5]. Those tests included several phases, from bench testing to a full 120 m beam path with feedback alignment which was subjected to motions typical of an ITER bake cycle. Over the course of the testing, the initial conceptual design was refined significantly and several issues were addressed and obstacles overcome. The controlled laboratory environment which was ideal for characterizing the system performance and improving the design can, however, be significantly different than that of an operating tokamak with its full range of nonidealities such as electrical noise, limited access, radiation, potentially large abrupt motion, pump noise, optical degradation, etc. Following lab tests, the TIP prototype was moved and installed on DIII-D with initial results presented here.

The TIP prototype makes a two-color interferometry[6–8] measurement at 10.59 μm and 5.22 μm using a CO_2 and Quantum Cascade Laser (QCL) respectively, while a separate polarimetry measurement of the plasma induced Faraday effect is made by launching collinear right-handed (RH) and left-handed (LH) waves at 10.59 μm[9,10]. In this configuration, each beam of the two-color vibration compensated interferometer with wavelength λ_i, experiences a phase shift ϕ_i due to vibration (V) and plasma with electron density n_e given by

$$\phi_i = r_e \lambda_i \int n_e dL + \frac{2\pi V}{\lambda_i} \tag{1}$$

where $r_e = 2.82 \times 10^{-15}$ m and m_e the electron mass. The line-integrated density measured by the two-color interferometer becomes

$$\int n_e dL = \frac{\lambda_{CO2}}{r_e(\lambda_{CO2}^2 - \lambda_{QCL}^2)} \left[\phi_{CO2} - \frac{\lambda_{QCL}}{\lambda_{CO2}}\phi_{QCL}\right] \quad . \tag{2}$$

The quantity that will be referred to in this document as the "vibration compensated phase" is given by

$$\phi_{int} = \left[\phi_{CO2} - \frac{\lambda_{QCL}}{\lambda_{CO2}}\phi_{QCL}\right] \quad . \tag{3}$$

[a)] Invited paper published as part of the Proceedings of the 22nd Topical Conference on High-Temperature Plasma Diagnostics, San Diego, California, April, 2018.

At low electron temperatures, the polarimeter experiences a phase shift (ϕ_{pol}), which is twice the Faraday rotation angle and is given by:

$$\phi_{pol} = 2C_p\lambda^2_{CO2}\int n_e\vec{B}\cdot d\vec{L} \quad , \tag{4}$$

where B is the local magnetic field, and $C_p = 2.62 \times 10^{-13}$ rad/T. The factor of 2 in the right-hand side of Equation 4 assumes a linear phase to Faraday rotation angle conversion and will be discussed further in Section III C. Note, the interferometric phase shift and Faraday rotation angles shown are given in the cold-plasma approximation.

Previous simulations of the expected TIP signals during a 15MA ITER baseline scenario discharge found that the maximum measured plasma induced interferometer phase shift corresponds to roughly ten full CO_2 fringes while the measured Faraday rotation angle is always less than a full fringe, eliminating any possible phase ambiguity[4]. Thus, in the event of a fringe skip in the interferometer system, the interferometer can be renormalized using the polarimeter measurement. Additionally, with the resolution demonstrated here, the polarimeter could potentially be used by itself for feedback control of density.

This paper describes the successful DIII-D TIP prototype installation, operational experience and measurements of DIII-D plasmas. Many additional details about individual components and the TIP measurement approach implemented here can be found in Reference[5].

II. DIII-D TIP PROTOTYPE INSTALLATION

The principle of operation and actual optical table layout (Figure 1) is very similar to that described previously[5]. Radiation from a single 10.59 μm CO_2 laser (frequency $\omega_0 = 2.8 \times 10^{13}$ Hz) is used to create both right-handed (RH) and left-handed (LH) circularly polarized radiation with a difference frequency of $\delta\omega = (\omega_2 - \omega_1)$ =4 MHz, (where $\omega_1 = 40$ MHz and $\omega_2 = 44$ MHz) that forms the Plasma Leg probe beam as well as horizontally polarized light with frequency ω_o (Reference Leg). The frequency shifting is accomplished using acoustooptic cells. Detector 1 signals at frequencies $(\omega_2-\omega_1)$ and ω_1 are compared to that of Detector 3 to obtain the Faraday rotation and interferometry phase shifts respectively. Separation of the plasma and vibration induced phase shifts in the interferometer measurement is accomplished by using a second co-linear QCL based interferometer operating at 5.22 μm where the phase of the 40 MHz signal from Detector 4 is compared to that of Detector 2.

A few modifications from the previous optical table layout[5] were necessary to accommodate the swapped positions of the reference and plasma legs. The new optical table layout is shown in Figure 1. Besides the swapped reference and plasma leg mirrors which steer the beams off the optical table, another notable difference is the addition of fiber coupled lasers for alignment. Additionally, a separate HeNe laser is coupled into the plasma leg via a Germanium window (Ge1) placed immediately before the 4X expander. As discussed previously[5], the entire top of the TIP optical table is enclosed by a temperature controlled box. Different from the air cooled amplifiers and water chillers used on the DIII-D interferometer and the previous long beam path testing, the DIII-D TIP prototype was converted to use all water cooled components. This approach is what is envisioned for ITER to avoid releasing significant amounts of heat into the TIP enclosure at ITER.

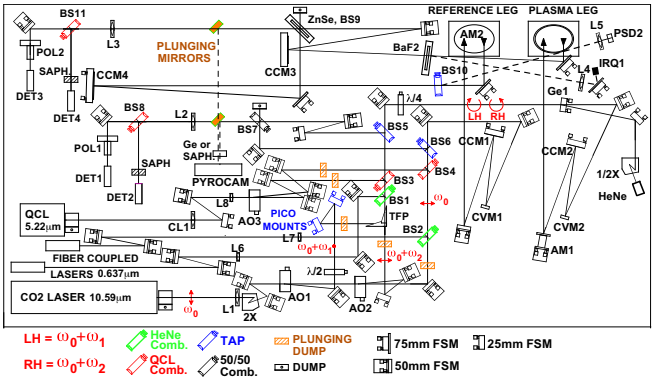

FIG. 1. TIP prototype table layout. Table is 1.2 m × 2.4 m. *Tap*= ZnSe beamsplitter, AO1, AO2, AO3 = Ge Acousto-Optic Modulator 40, 44, 40 MHz, $\lambda/2$ = CdS half-wave plate, *HeNe Comb.*= ZnSe beam combiner, *TFP* = ZnSe thin film polarizer, $\lambda/4 = 10.59\,\mu$m CdS quarter-wave plate, *QCL Comb.*= ZnSe beam combiner, 50/50 *Comb.*,= ZnSe beamsplitter, *DET*= HgCdTe PV detectors, *Pol* = 10.59 μm ZnSe Brewster Angle Based Polarizer, *FSM* = front surface mirrors, *L*1 =25.4 cm FL ZnSe lens, *L*2 and *L*3=50 cm FL ZnSe lens, *CL*1=-1.2 m FL CaF2 cylindrical lens, *Pyrocam* = Ophir Pyrocam^{TM} beam profiler.

The DIII-D TIP prototype features 96 m roundtrip beam paths on both the reference and plasma legs as shown in Figure 2a. The plasma leg enters DIII-D through a midplane radial port where it is steered toroidally by a large angle of incidence copper mirror placed inside the vacuum vessel (See Figure 2b). The beam then travels across the vessel midplane with a tangency radius of $R_{tan} = 1.19$ m until it strikes a titanium retroreflector that is intentionally manufactured such that the incoming and outgoing beams are at an angle of 0.131 Deg. with respect to one another. Similar to the current ITER design, this angular offset causes the beams to overlap at the location of the copper mirror when separated vertically by 1 cm on the CCR.

As in Reference[5], the 96 m reference and plasma leg path lengths were matched using the QCL in pulsed mode to measure the difference, then adjustments were made to the reference leg. Final fine tuning of the alignment as well as wavelength calibration is then carried out using a CCR on translation stage. For these studies, the refer-

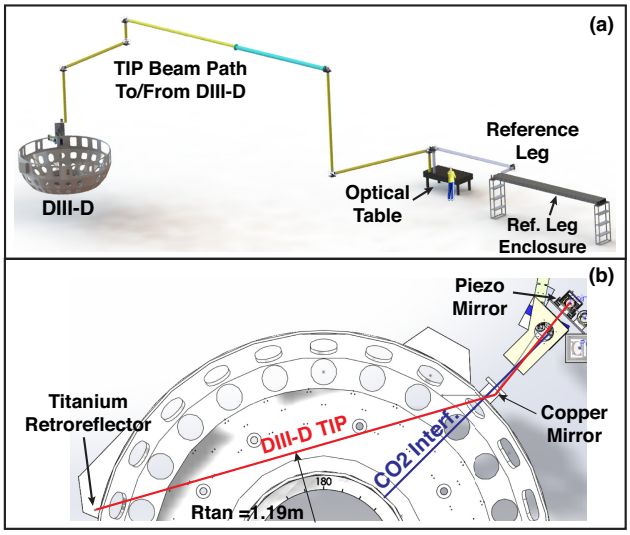

FIG. 2. (a) Overall TIP prototype layout and beam paths on DIII-D. (b) Plasma leg beam path through DIII-D midplane.

ence and plasma leg path lengths are matched to within approximately 1 cm which lowers interferometer phase noise arising from the finite QCL linewidth[5].

In addition to aligning the beam path components off the table, the TIP has several co-alignments that must be carried out on the optical table. The RH and LH 10.59 μm beams on the plasma leg must be aligned collinear to one another and the 5.22 μm QCL beams must be aligned collinear to the plasma and reference leg CO_2 beams. As was discussed in the previous work[5], a camera based approach was developed to simplify and improve this process beyond previous approaches which used luminescent plates. This approach uses Picomotor remote controllable mounts and remotely actuated beam dumps combined with plunging mirrors to remotely align one beam at a time as the different beams are cycled through and directed to the Pyrocam beam profiling camera (Figure 1) in the near and far field.

Each leg of the DIII-D TIP is completely enclosed, but not air tight. The plasma leg uses 150 mm diameter aluminum piping for the majority and, at each turn, the 150 mm diameter mirrors are enclosed in an aluminum box. The majority of the reference leg is enclosed in a single wide duct (See Figure 2a), in which the beams travel back and forth for a total of ten small angle of incidence passes - this approach minimizes optical components, losses and overall footprint. The plasma leg turning mirrors are the same zero phase shift mirrors as used in the previous long beam path prototype[5] and the reference leg mirrors are protected silver.

A. DIII-D BaF_2 Windows

As currently envisioned for ITER, the DIII-D TIP uses BaF_2 primary vacuum windows as well as for beam sampling to carry out feedback alignment. BaF_2 is a good window choice due to the facts that it can be polished to excellent optical tolerances and that it has a low Verdet constant; however, BaF_2 has significant absorption at the primary measurement wavelength of 10.59 μm with approximately 13%/cm. The DIII-D TIP plasma leg passes through three double-pass BaF_2 windows before returning to the optical table - a 7.6 mm thick, 91.4 mm diameter beam sampling window, the primary vacuum window (11.6 mm thick, 140 mm diameter), a protective window inside the vacuum (7.6 mm thick, 91.4 mm diameter) and then a return through each after being reflected by the CCR. The total calculated double-pass window transmission including reflection losses is 34% and the total calculated table-to-table transmission, which includes all optical elements off of the optical table itself, is 17%.

The DIII-D TIP uses a ≈7.5 W Infrared Instruments 10.59 μm CO_2 laser. After all of the splitting, right and left-handed polarization preparation, expansion, etc., approximately 1.5 W is launched off the table on the plasma leg. This corresponds to roughly 250 mW of return power, with the majority of the power being lost to the three BaF_2 windows. This level of return power is actually marginal for alignment purposes and more power would be optimal for the ITER implementation which has comparable expected losses.

B. DIII-D TIP Data Acquistion (DAQ) and Monitoring Software

The TIP DAQ and demodulator is very similar to the system implemented in the previous lab testing phase[5] with revisions to accommodate the DIII-D shot cycle, MDSPlus data storage, and simultaneous data storage rates of 500 kS/s and 10 kS/s. The TIP DAQ is essentially a digital phase demodulator (DPD) built around an FPGA interfaced to four high-speed ADCs. The DPD measures the phase shift of three intermediate frequency signals (4, 40, and 44 MHz) from two different CO_2 laser detectors and a 40 MHz signal from two different QCL detectors on the optics table with a demonstrated instrumental phase resolution of $\delta\phi$ <0.01 Deg. with 500 kHz useable bandwidth and $\delta\phi$ <0.002 Deg. with 1 kHz bandwidth. The actual FPGA unit, amplifiers, DC blocks, etc. are packaged in a rack mounted case. A key feature of the TIP DAQ system is a real-time selectable "scope" which displays the various phase traces as well as a signal levels, and statistics on the measured signals.

For the DIII-D TIP implementation, monitoring of several key signals has been incorporated into the TIP DAQ system and is used for troubleshooting and evaluation of system performance. Examples of signals monitored continuously at 1 Hz are: Thermocouples inside and out-

side of the optical enclosure, piezo drive voltages, position sensor voltages, magnitude of all interference levels for each laser (40, 44, 4 MHz for CO_2 and 40 MHz for QCL), water flow, water temperature, wavelength, etc. These additional signals are essential to understanding the behavior during a discharge and the various sources of noise as well as troubleshooting when issues arise.

C. Feedback Alignment

As was found in the previous lab testing phase, feedback alignment is also an essential component of the DIII-D TIP prototype. A diagram showing the basic feedback scheme for both the plasma and reference legs is given in Figure 3. Very similar to the lab testing, the plasma leg has two active feedback circuits, with one active mirror on the TIP optical table (Labeled AM1 in Figure 1) and another at the vessel. The second active mirror location near the DIII-D entrance window is labeled in Figure 2. The active mirror on the TIP optical table (Newport PSM2 with 50mm x 50mm protected silver square mirror) is controlled by a position sensor immediately before the active mirror shown in Figure 2b; essentially, the active mirror on the TIP optical table keeps the beam fixed at the DIII-D vessel position sensor and the piezo mirror (PI S-340 with a 100 mm diameter protected silver circular mirror) at the vessel keeps the beam fixed at a point on the optical table by a second position sensor (Labeled IRQ1 in Figure 1). Originally, this position sensor was a Thorlabs visible laser position sensor but later, was changed to a HgCdTe CO_2 laser quadrant sensor as is envisioned for ITER. The beam sampling at the vessel is carried out by a separate uncoated BaF_2 window which is the same as that used in the previous lab tests[5].

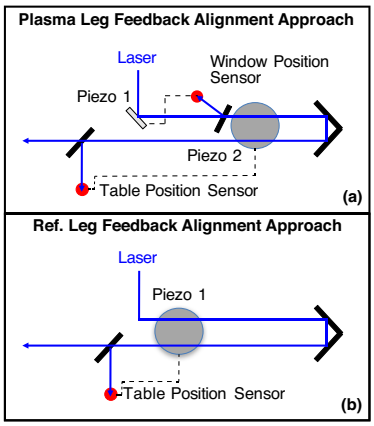

FIG. 3. DIII-D TIP feedback alignment approach for (a) plasma and (b) reference legs respectively.

III. DIII-D TIP TEST RESULTS

A. Measurement Noise Floors

DIII-D TIP equilibrium density profile measurements were found to be low noise and able to meet ITER density measurement requirements from early in the commissioning phase. Figure 4 shows an example TIP measurement of a DIII-D plasma, where vibration compensated phase noise floors are $\delta\phi_{int} \approx 1$ Deg. and polarimeter noise is $\delta\phi_{pol} \approx 0.03$ Deg. respectively. The implied line-integrated density resolution for the vibration compensated interferometer is δnL=1.5×10^{17} m^{-2} and the magnetic field weighted line-integrated density from the polarimeter is δnBL=1.5×10^{19} Tm^{-2}. The actual differential path length variation (i.e. the "vibration") is also shown in Figure 4a. The peak to peak variation is ≈ 1.2 mm during the particular discharge shown, which corresponds to 8.3×10^4 Deg. for the QCL yet the interferometer noise is of the order of 1 Degree. This vibration value depends on current, toroidal field, Ohmic coil ramp rate, etc. but nonetheless, it is well compensated. For reference, to meet ITER measurement targets with either the interferometer or polarimeter, a vibration compensated phase error of $\delta\phi_{int} < 10$ Deg. and a polarimeter

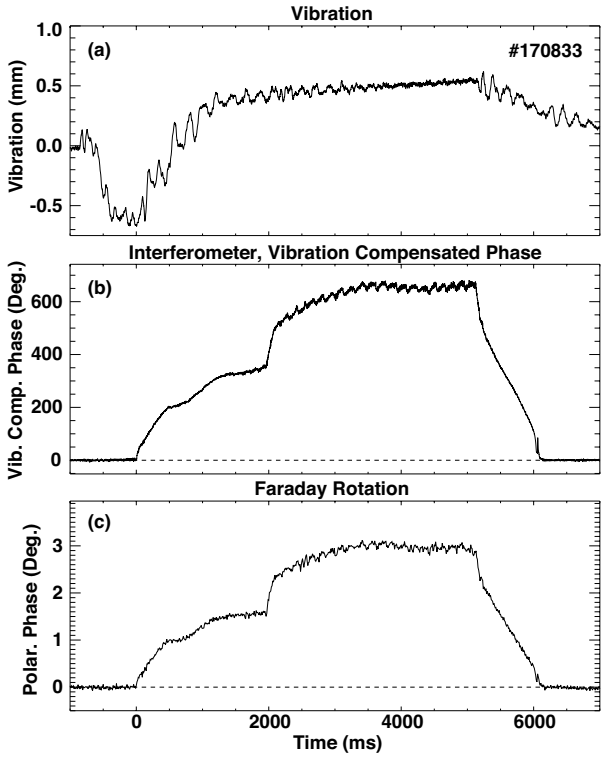

FIG. 4. DIII-D TIP prototype measurements of discharge #170833. (a) Measured physical path length change between reference and plasma legs, i.e. "vibration". (b) Interferometer measured vibration compensated phase. (b) Polarimeter measured Faraday rotation induced phase shift.

error of $\delta\phi_{pol} < 0.1$ Deg. are required. An analysis of DIII-D TIP data from over 250 DIII-D discharges taken in May to June 2017 shows an average $\delta\phi_{int} = 1.9$ Deg. with 1 kHz bandwidth and $\delta\phi_{pol} = 0.05$ Deg. with 100 Hz bandwidth. Further, these measurements compare well with expectations as will be shown in Section III B.

The measured TIP interferometer noise floor on DIII-D is consistent with that found in the previous long beam path studies and is primarily affected by residual transverse motion as well as, to a smaller degree, the finite linewidth of the QCL laser. Residual transverse motion contributes to vibration compensated interferometer errors primarily in two ways. All windows are manufactured with some wedge; when the two-color interferometer beams move across wedged windows, or any transmissive element, there is a differential phase shift between the different wavelengths due to dispersion in the medium. The system is designed such that the transmissive elements are located near beam positions that are nominally fixed, i.e. at the vessel window and back on the optical table, but if the beam moves on the order of millimeters, this motion combined with the specified level of wedge in the various components, can cause degree level phase errors. Transverse motion can also cause interferometer errors due to the fact that the interfering reference and plasma legs have some curvature to their phase fronts which is different for the two colors. This phase front curvature combined with transverse motion causes uncompensated phase shifts. Transverse motion

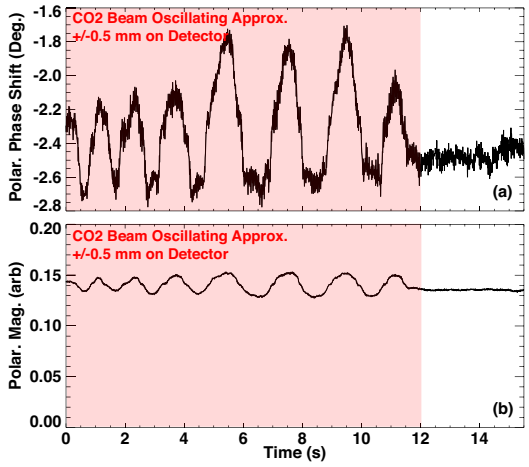

FIG. 5. Polarimeter phase shift and magnitude as the CO_2 beam position on the final detector is varied.

is the single largest source of noise for the polarimeter. If the launched R and L waves are not perfectly collinear, differential vibration and plasma induced phase shifts can dominate the relatively small polarimeter signal. As discussed in Reference[5], transverse motion on the plasma leg CO_2 detector also causes an unwanted phase shift of the polarimeter. An example of this is given in Figure 5, where the final mirror before the polarizer/detector on the plasma leg is manually oscillated causing approximately a +/- 0.5 mm displacement on the 4mm x 4mm detector. The result is an approximately 0.3-0.5 Deg. oscillation in the polarimeter phase signal (or 3-5X the total polarimeter error budget). The exact cause of this error is not yet well understood but it can be made worse with poor R and L wave co-alignment as well as beam distortion.

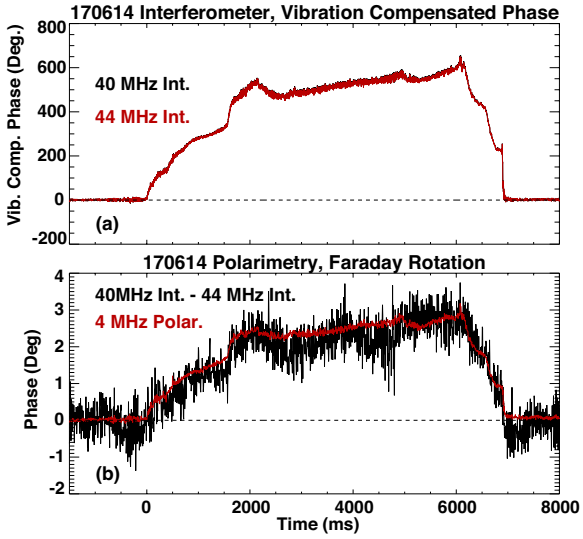

FIG. 6. (a) 40 and 44 MHz vibration compensated phase. (b) Faraday rotation inferred from 4 MHz polarimeter (red) and from taking the difference of the 44 and 40 MHz vibration compensated interferometer signals.

The TIP actually makes two vibration compensated interferometer measurements, one system uses the R-wave at 40 MHz and the other uses the 44 MHz L-wave at 10.59 microns. The typical expression for the interferometric phase shift given in Equation 1 uses the average of the R and L-wave index of refraction, while the Faraday rotation in Equation 4 results from the difference of the two.[12] The polarimeter interferes overlapping R and L-waves to measure the differential phase shift (4 MHz Demodulation) and ultimately infer the Faraday rotation. In principle, the Faraday rotation can also be obtained by taking the difference of the R and L wave interferometer phase shifts (40 and 44 MHz Demodulation). A comparison of the two approaches is given in Figure 6. Figure 6a shows the 40 and 44 MHz vibration compensated interferometer measurements which are both low noise and essentially overlapping on the scale shown. The difference of the 40 and 44 MHz CO_2 interferometric phase signals is shown in Figure 6b along with the 4 MHz polarimeter phase shift. The signals are similar, however, the 4 MHz polarimeter noise is approximately an order of magnitude lower. The fact that the signals are similar is encouraging since it validates our interpretation of the measurement. The increased noise is perhaps to be expected for a couple of reasons, one of which is that 40-44 MHz approach requires taking the difference of two large numbers on the order of 10^4 Degrees to arrive at

phase shifts on the order of 1 Degree. The polarimeter noise in Figure 6b is $\delta\phi_{pol} = 0.03$ Deg. and 0.4 Deg. from the difference of the 40 and 44 MHz CO_2 phase signals.

TIP will not only be used to measure line-integrated density but it will also fulfill a secondary requirement for the measurement of core density fluctuations from turbulence, Alfvén eigenmodes, sawteeth and other MHD. Like the standard DIII-D vibration compensated CO_2 interferometer, TIP is a sensitive fluctuation diagnostic. Figure 7 shows a TIP interferometer spectrogram during a discharge with a range of coherent mode activity. Two types of Alfvén eigenmodes, the Beta Induced Alfvén Eigenmode (BAE) and the Reversed Shear Alfvén eigenmode (RSAE) are identified as are neoclassical tearing modes (NTM). These low noise measurements allow clear identification of the core fluctuation activity, something that will be invaluable for the TIP on ITER.

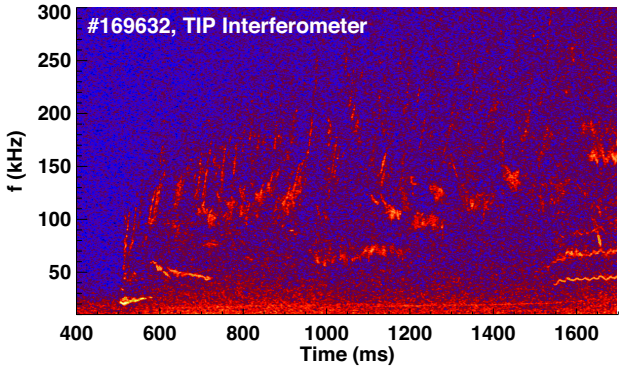

FIG. 7. TIP 40 MHz interferometer spectrogram showing range of coherent and semi-coherent fluctuations.

In addition to higher frequency fluctuations like AEs, low frequency fluctuations or slow MHD are also clearly resolved by TIP. As an example, Figure 8 shows TIP measurements of sawteeth in an ITER baseline scenario plasma.

B. Measurement Accuracy

The TIP vibration compensated interferometer measures line-integrated density along the sightline (Eqn. 2) and the polarimeter measures a similar line-integrated quantity that is weighted by the local magnetic field parallel to beam propagation (Eqn. 4). To check the accuracy of the measurement, a synthetic diagnostic was written which takes as inputs EFIT[13] magnet equilibrium reconstructions and fits to Thomson scattering measured density profiles. Density profiles are mapped to real space and the line integral is calculated piecewise along both the TIP sightline and, for an independent check, the DIII-D radial interferometer sightline. Similarly, polarimeter signals are simulated using the local magnetic field calculated from EFIT combined with the density profile. Figure 9 and Figure 10 show these measurements

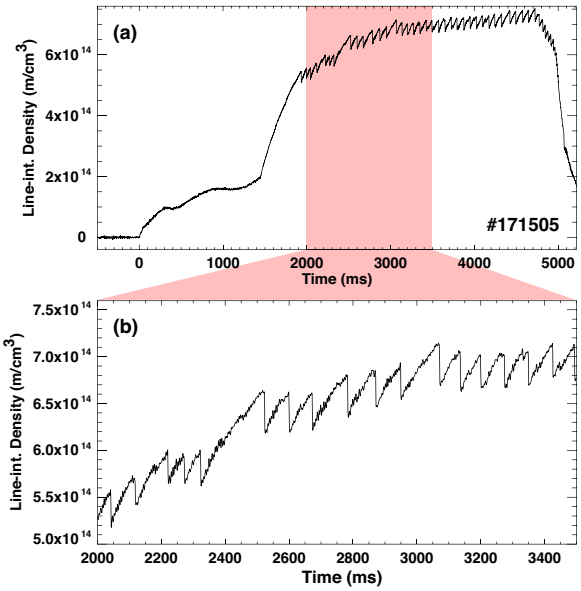

FIG. 8. TIP measurements of sawtooth induced density oscillations.

agree well with expectations for both the polarimeter and interferometer respectively. Additionally, Figure 9 compares two separate discharges taken with different toroidal field (Bt) directions and shows the polarimeter measured phase shift exhibits the expected change of sign.

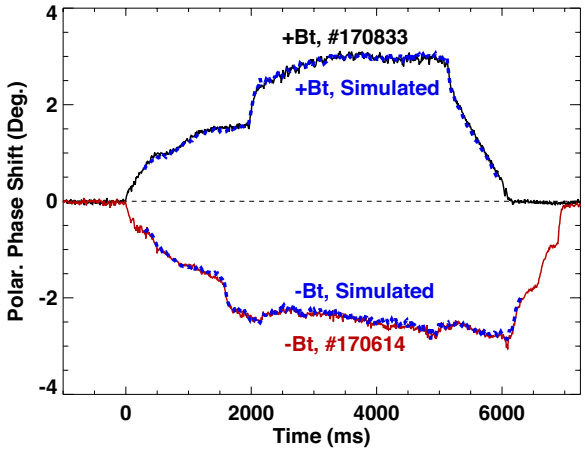

FIG. 9. Polarimeter measurements in +/-Bt compared to expectations (blue).

As shown in Figure 10 the TIP interferometer noise floor is typically lower than that of the DIII-D vibration compensated interferometer (a 10.59 and 3.39 μm based system) that is used daily for feedback control of density. Due to the longer path length, the TIP interferometer phase shift is also $\approx 3X$ that of the DIII-D radial chord.

Since both the equilibrium reconstruction and Thomson profile fitting process have their own uncertainties, the question of how well the expected TIP signals agree

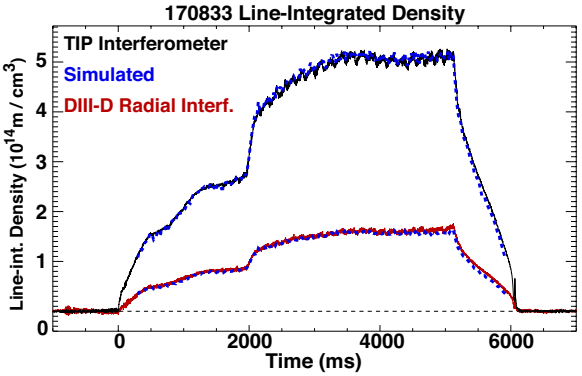

FIG. 10. TIP Interferometer measured line-integrated densities (black), DIII-D radial interferometer measurements (red) and simulations (blue).

with predictions is examined more closely. Two-color interferometer measurements such as TIP are common and accepted. The error is well approximated by looking at noise floors before $t = 0$ (i.e. when there is no plasma), as were quoted in the previous section. The CO_2 laser R and L wave polarimeter, on the other hand, is far less common and significant disagreement with expectations have been found in LHD plasmas[9]. To get at the question of whether the polarimeter agrees with expectations, data from over 500 DIII-D discharges were filtered down to times for which simulated line-integrated densities agreed with DIII-D radial interferometer and TIP interferometer measurements to within 5%, this criteria was used to remove fits for which the EFIT / Thomson profile fitting process introduced errors and/or the system was experiencing other issues associated with the commissioning process. The result is a comparison of data/simulation from 251 discharges and $\approx$ 24,000 EFIT time slices. This comparison showed an average fractional difference between polarimeter simulations and measurements of $\delta\phi_{pol}/\phi_{pol} = 4\%$ and a corresponding average phase difference of $\delta\phi_{pol} = 0.07$ Deg. These results are extremely encouraging and show the TIP polarimeter is functioning as expected.

C. Calibration

To convert the measured phases into line-integrated density and Faraday rotation, at low electron temperatures, TIP needs essentially two calibration factors. For line-integrated density from the two-color interferometer, the wavelength ratio of the two probe lasers is essential (See Eqn. 2). For converting polarimeter phase to Faraday rotation, a conversion factor is required - in Eqn. 4, this is the source of the factor of 2.

For gas lasers in the wavelength range of interest, the wavelength ratio can typically be assumed fixed. If vibration is large, the constraint on this ratio is $\approx$ 1 part in 10^5 causes a 1 degree phase error in the presence of 2 mm motion. For the QCL used, however, it was not a-priori obvious whether this factor could be assumed fixed. To deal with this the same approach as described in Reference[5] was employed; a remotely translatable retroreflector was added to the reference leg. Before each discharge, the retroreflector was programmed to move 1 mm then, after the discharge, it moved back. The effect of this was to always add some known motion before and after such that the wavelength ratio could be determined by adjusting it to remove this motion from the vibration compensated signal. For phase shifts of 10^5 Degree the vibration compensated phase is cancelled with a residual error on the degree level, assuming a wavelength ratio of $\lambda_{QCL}/\lambda_{CO2} = 0.493013$ with $\lambda_{CO2} = 10.591$ μm and $\lambda_{QCL} = 5.22150$ μm . The polarimeter phase shows no evidence of the motion and is significantly < 0.1 Degrees.

Over 547 discharges with interferometer data, the inferred wavelength ratios from minimizing the vibration compensated phase shift before $t = 0$ was $\lambda_{QCL}/\lambda_{CO2} = 0.49305 \pm 8 \times 10^{-5}$, representing an error of 1 part in 10^{-4}. These numbers are very encouraging since this is the variation over an approximately three month period. Typical inter-shot variation will be significantly smaller as was observed in previous lab testing. Also, QCLs with an order of magnitude better line stability are available and will be used for the ITER implementation.

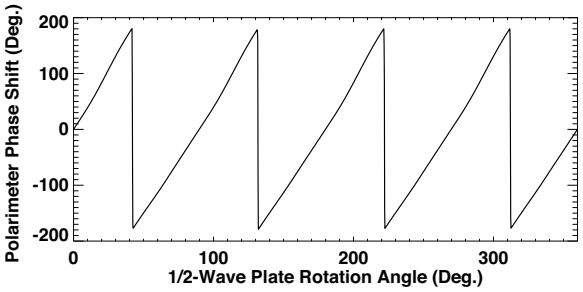

FIG. 11. Polarimeter phase as a 1/2 wave plate is rotated 360 Deg.

The polarimeter phase to Faraday rotation conversion can be as simple as a constant factor of 2 or can be dependent on phase. A phase dependent conversion factor is required if the launched polarization is elliptized either due to poor preparation of the R and L waves or, possibly coatings and other optical surface degradation that can occur over time. To measure the conversion factor, typically a half-wave plate is inserted in the beam path and rotated[11]. When the half-wave plate is rotated, the 4 MHz polarimeter phase shift should be 4X the rotation angle and linear with rotation angle. Any deviations from 4X can be taken into account using a linear fit to phase vs. rotation angle curve or, depending on how severe the degradation is, the actual curve itself can be used. In practice, a complication is that the wave plate itself can introduce some unwanted nonlinearity as well.

To test the conversion from polarimeter phase to Faraday rotation angle, a half-wave plate was inserted in vary-

ing locations on the optical table and rotated by 360 degrees. An example of the measured polarimeter phase shift of the 4 MHz interference signal when the half-wave plate is placed immediately before lens L3 (See Figure 1) is shown in Figure 11. One can see there are four cycles for one full rotation of the half-wave plate. Also, not shown is the fact that magnitude is also being modulated slightly with the same periodicity. Further, the shape of the polarimeter phase from -180 to 180 deg. vs. wave plate rotation angle appears repeatable and deviates slightly from linear in each quarter rotation. A linear fit to the unwrapped signal has a slope of 3.99 which is within 0.3% of the nominal 4.

IV. FEEDBACK ALIGNMENT CONSIDERATIONS

As mentioned, feedback alignment for TIP is essential. Figure 12 shows DIII-D TIP measurements in a series of discharges (not necessarily identical repeats) with various parts of the plasma leg feedback alignment system disabled, and the corresponding impact on measurement quality. Note, for measurements with some portion of the alignment system disabled, all components were kept in closed loop mode until 20 s before each discharge, at which point the corresponding systems were put in open loop mode. This approach ensured that beams were centered on their corresponding detectors at the beginning of each discharge.

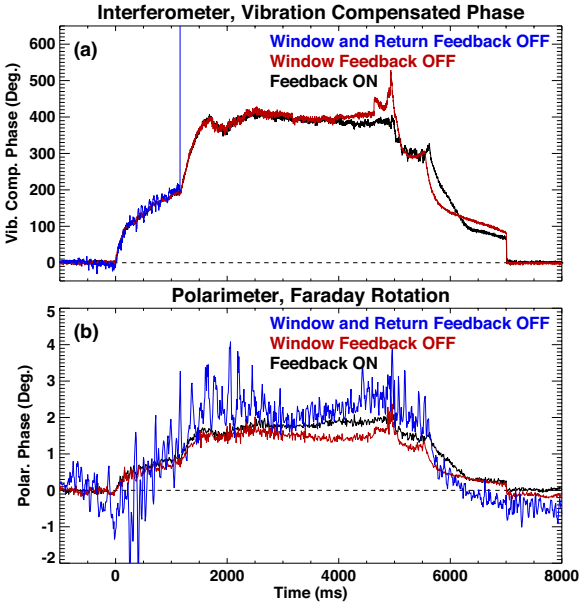

FIG. 12. TIP measurements with various parts of the plasma leg feedback alignment system disabled. Blue = NO feedback alignment on the plasma leg. Red = window feedback alignment is off. Black = Feedback alignment ON. NOTE: These discharges are not identical repeats and the data should NOT overlay exactly, but comparisons of the noise are useful.

The results shown in Figure 12 are extremely useful for several reasons. First, the results with both circuits of the plasma leg feedback alignment system disabled (blue) show unacceptably large increases in both the interferometer and polarimeter phase noise relative to the measurements with both systems enabled (black). With no feedback alignment, during a DIII-D discharge, the vibration compensated interferometer noise increases to 20+ Degrees then the measurement suffers a fringe skip after only 1200 ms of the 7000 ms discharge. The polarimeter noise also increases substantially with noise rising to the degree level. With only the "window" feedback circuit disabled during a discharge (red), however, the results are quite different. In this configuration, the beam position after returning to the optical table is held fixed by the piezo mirror near DIII-D but the piezo mirror on the optical table, which would normally hold the beam fixed at the DIII-D position sensor, is held fixed. The results of this test show very similar noise floors can be maintained for both the interferometer and polarimeter even with the window portion of the feedback alignment system locked.

If the window circuit of the feedback alignment system can be locked during a discharge, this has significant positive design implications for the ITER TIP implementation. In the current design, one potential point of failure on ITER during high radiation discharges is the position sensor located near the device. If the system is only required to slowly maintain alignment throughout the day as temperature variations occur, but is not required to be active during a discharge, the position sensor can be replaced with a single radiation hard optical fiber and detector based solution. While a single intensity-based feedback alignment system is slower and requires dithering, it's inconsequential because the system could simply ensure the beam is centered on the ITER window before a discharge begins then, stay fixed during the actual discharge.

One of the largest sources of polarimeter noise, and to a lesser degree interferometer noise, appears to be motion due to mechanical resonances of the piezo mirror tip/tilt stage near the DIII-D vessel. For the DIII-D prototype, this resonance is at 205 Hz and can be excited by impulsive forces/fields during a discharge as shown in Figure 13. This motion cannot be compensated for by the feedback alignment system and has several important implications for the measurement and design:

- If possible, all mechanical resonances of the piezo mirrors should be above the required measurement bandwidth.
- A higher frequency requirement pushes the design to smaller/lighter piezo mirrors. For example, the 100 mm glass mirror in the current design can be replaced by a 75 mm mirror made of glass or even potentially beryllium.
- A non-magnetic tip/tilt stage should be used to avoid magnetic forces exciting the resonances (the D3D TIP prototype tip/tilt platform is magnetic).

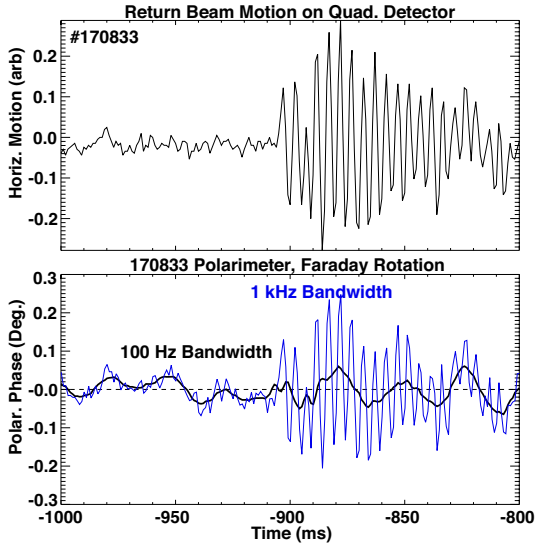

FIG. 13. The impact of motion on polarimeter noise, note, this is the same discharge as Figure 16. (a) Motion of the return beam. (b) Polarimeter phase with 100 Hz (black) / 1 kHz (blue) bandwidth.

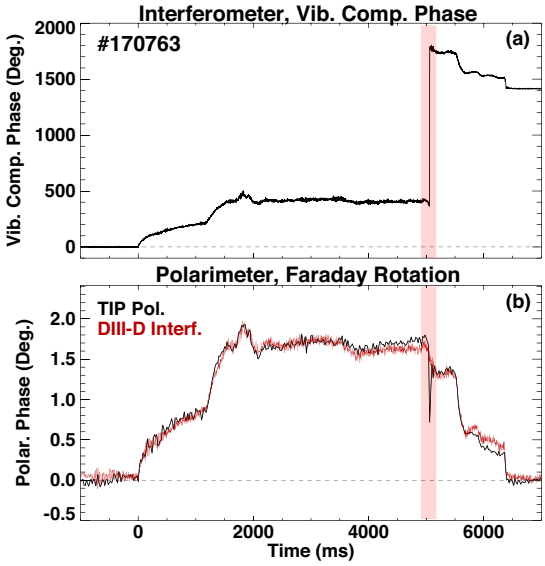

FIG. 14. (a) TIP interferometer phase showing a fringe skip due to signal loss. (b) TIP polarimeter phase (black) and DIII-D radial interferometer trace (red).

- If the motion becomes large enough, the beams can come off the detector and dropout occurs. This pushes the design towards larger detector elements.
- The largest impact on the measurement is increased noise on the polarimeter due to motion on the detector. This effect is not currently understood.
- This resonance induced motion can contaminate vibration compensated interferometer measurements through dispersion in wedged transmissive components

As mentioned, a consequence of rapid motion that cannot be tracked is that momentary signal loss can occur leading to interferometric fringe skips. An example of this is shown in Figure 14a. Fortunately, immediately after the brief signal loss, the polarimeter signal recovers without a fringe skip since its phase shifts are always less than 2π and the signal could then be used to recover the interferometer phase. For reference, the radial DIII-D interferometer chord trace is shown overlayed on the polarimeter trace in Figure 14b to show it indeed should recover to the value it does.

V. CONCLUSIONS

A CO_2 and QCL based TIP prototype has been installed and tested on the DIII-D tokamak. Both the interferometer and polarimeter signals agree with expectations, are low noise and are capable of meeting ITER's density measurement requirements. An active feedback alignment system has also been tested and found to be an essential element of the TIP. Future work will include improving the feedback alignment response as well as potentially a change to a higher power, narrower linewidth 4.6 μm QCL to increase signal, improve phase resolution and avoid any atmospheric interaction.

VI. ACKNOWLEDGEMENTS

This work is supported by U.S. DOE Contract numbers DE-AC-02-09CH11466 and DE-FC02-04ER54698. PPPL Prime Contract Number is DEAC-02-09CH11466. All US TIP activities are managed by the US ITER Project Office, hosted by Oak Ridge National Laboratory with partner labs Princeton Plasma Physics Laboratory and Savannah River National Laboratory.

VII. DISCLAIMER

the United States Government or any agency thereof.

[1]A. J. H. Donne, A. E. Costley, R. Barnsley, et. al. Nucl. Fusion **47**, S337 (2007).
[2]T. N. Carlstrom, *et al.*, "Baseline Design of a Multi-channel Interferometer and Polarimeter System for Density Measurements on ITER," Diagnostics for Experimental Thermonuclear Fusion Reactors 2, Edited by Stott *et al.*, Plenum Press, New York (1998).
[3]T. Kondoh, *et al.*, Rev. Sci. Instrum. **75**, 3420 (2004).
[4]M. A. Van Zeeland, R. L. Boivin, D. L. Brower, T. N. Carlstrom, *et.al.* Rev. Sci. Instrum. **84**, 043501 (2013).
[5]M.A. Van Zeeland, T.N. Carlstrom, D.K. Finkenthal, R.L. Boivin, A. Colio, D Du, *et.al.* Plasma Phys. Controlled Fusion **59**, 125005 (2017).
[6]M. A. Van Zeeland, R. L. Boivin, T. N. Carlstrom, T. Deterly, D. K. Finkenthal, Rev. Sci. Instrum. **77**, 10F325-1 (2006).
[7]T. N. Carlstrom, D. R. Ahlgren, and J. Crosbie, Rev. Sci. Instrum. **7**, 1063 (1988).
[8]Yasunori Kawano, *et al.*, Rev. Sci. Instrum. **67**, 1520 (1996).
[9]T. Akiyama, *et al.*, Rev. Sci. Instrum. **74**, 2695 (2003).
[10]M. A. Van Zeeland, *et al.*, Rev. Sci. Instrum. **79**, 10E719 (2008).
[11]D. L. Brower, *et al.*, Rev. Sci. Instrum. **72**, 1077 (2001).
[12]W. X. Ding, *et al.*, Rev. Sci. Instrum. **74**, 3387 (2004).
[13]L. L. Lao, H. E. St. John, R. D. Stambaugh, A. G. Kellman, and W. Pfeiffer, Nucl. Fusion **25**, 1611 (1985).